ACEEE Int. J. on Electrical and Power Engineering, Vol. 4, No. 1, Feb 2013

Analysis and Control of Wind Driven Self-Excited Induction Generator for Isolated Applications

M.Sathyakala[1], M.Arutchelvi[2]
[1]Saranathan College of Engineering/EEE, Trichy, India
Email: muthuvelsathya@yahoo.com
[2]Saranathan College of Engineering/EEE, Trichy, India
Email: arutchelvi@gmail.com

***Abstract*—For isolated applications, the 3-Φ self-excited induction generator driven by wind energy source is more suitable, where the minimum excitation capacitance required for self-excitation of 3-Φ induction generator is taken up in this work and the detailed analysis is carried out to determine the range of wind speed variation and consumer demand for the designed capacitance value. An electronic load controller is designed to maintain the load voltage constant for these variations. The excess power resulting as a consequence of rise in load voltage due to variation in load is pumped to dump load along with battery storage. Simulation for battery feeding the consumer load in the absence of wind power has been undergone. Exhaustive simulations have been carried out for such a scheme and the results have been presented in this paper.**

***Index Terms*— wind energy source, self-excited induction generator, electronic load controller, chopper, dump load, lead-acid battery.**

I. Introduction

From Ref. [1], Ref. [2], Ref. [3] the permanent magnet synchronous generator (PMSG) is particularly an attractive option in renewable energy applications, but the permanent magnets are quite expensive, demagnetization of permanent magnet at high temperature and torque, current, MMF vectorially combines with persistent magnetic flux of permanent magnets, which leads to higher air-gap flux density and eventually, leads to core saturation. Another disadvantage of PMSG is that uncontrolled air-gap flux density leads to over voltage and poor electronic control reliability. From Ref. [4], Ref. [5] the induction generator (IG) is the most common generator in wind energy system applications in the stand-alone systems due to its simplicity and ruggedness, more than 50 years life time. The interest in this topic is primarily due to the application of self-excited induction generator (SEIG) in isolated power systems where a capacitor bank is connected across the stator terminals, which provides the required excitation for SEIG. From Ref. [6], Ref. [7] some of its advantages are small size and weight, robust construction, absence of separate dc source for self-excitation and reduced unit and maintenance cost. Due to the brushless construction, low maintenance and low capital cost SEIG gives an important advantage over the synchronous generator. The terminal capacitance on such machines must have a minimum value so that self-excitation is possible. Due to the brushless construction, low maintenance and low capital cost SEIG gives an important advantage over the synchronous generator. The SEIG requires minimum excitation capacitance for self-excitation which provides lagging reactive power of both IG as well as load. From Ref. [7], Ref. [8], Ref. [9], Ref. [10], Ref. [11], Ref. [12] the design of excitation capacitance depends upon mainly on the magnetizing reactance and per unit frequency. Although, all numerical results yields the solution for general R-L case, initial guessing of magnetizing reactance and per unit frequency is required, tedious and lengthy derivations are involved. In Ref. [10] a simple method and direct method for computing the minimum value of excitation capacitance required for initiating voltage build up in a 3-Φ SEIG under R-L load is presented.

In this paper, the 3-Φ stand-alone wind-driven SEIG with an electronic load controller (ELC) feeding R-L load is undergone where the self-excitation capacitance is calculated by using direct method. In section 2, the brief description of the system is explained. In section 3 and 4, the design of self-excitation capacitance and ELC has been developed. In section 5 modeling and design of lead-acid battery is explained. In section 6, by using MATLAB software the simulation results of SEIG with an ELC feeding 3Φ consumer (R-L) load and dump load with battery and battery feeding the consumer load in the absence of wind power is shown. The simulation for variation in wind speed of SEIG feeding constant 3Φ R-L load with the designed self-excited capacitance is shown.

II. Block Schematic Description

The schematic arrangement of the proposed stand-alone power generation scheme with SEIG is shown in Fig.1. The proposed scheme consists of the 3- Φ IG (3HP, 2.2kW, 380V, 5.5A, 50Hz) driven by a wind turbine, excitation capacitor bank along with ELC, which consists of a 3-Φ diode-bridge rectifier fed chopper circuit with dump load along with battery and the 3- Φ R-L load. Suitable values of self-excitation capacitors are connected across the SEIG such that it generates rated terminal voltage at full load.

Since, the input power is nearly constant, the output power of the SEIG is held constant at varying consumer loads. The power in surplus of the consumer load is dumped in a dump load through the ELC. The ELC consists of a 3-Φ uncontrolled rectifier with a chopper in series with a dump load.

The ELC with chopper switch has the advantages of which, only one switching device is needed and so the

DOI: 01.IJEPE.4.1.1122

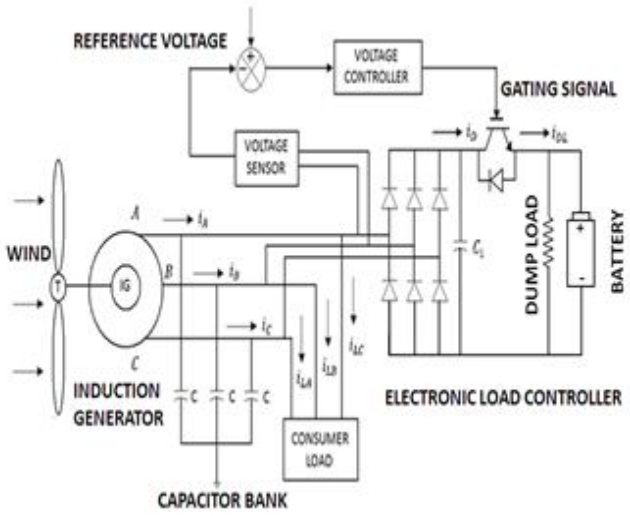

Figure 1. Schematic diagram of the 3 Φ SEIG with an ELC feeding three-phase consumer load

driving circuit is required for the chopper switch alone and so, the scheme is very simple, cheap, rugged and reliable, low value of generation of harmonics and no reactive power demand and requires only one dump load and hence, it is inexpensive and compact.

Thus, SEIG feeds two loads in parallel such that the total power is constant, that is,

P_{out} (generated power which should be kept constant)=P_c (consumer load power)+P_d(dump load power).

III. Design Of Excitation Capacitance For 3-Φ Seig

The typical parameters for 3-Φ IM such as R_s=4.8Ω ,R_r=5.77Ω , X_{ls}=X_{lr}=15.66Ω , X_m=230Ω are estimated by conducting no-load test and blocked rotor test experimentally in the laboratory.

The load parameters such as the resistance (R=25 Ω) and the inductance (L=100mH) are calculated by considering the rated value of voltage and current of the 3- Φ IM.

In Fig. 2The per phase steady-state circuit of 3- ΦSEIG under R-L load is shown. where R_s, R_r, R, X_{ls}, X_{lr}, X, X_m, X_{smax} = per unit per phase stator, rotor (referred to stator) and load resistance, stator leakage and leakage (referred to stator) load and magnetising reactances (at base frequency) and maximum saturated magnetising reactance, C = per phase terminal-excitation capacitance , X_c = per unit per phase capacitive reactance (at base frequency) of the terminal excitation capacitance , F, v = per unit frequency and speed, N, f_b, Z_b= base speed in rev/min, base frequency, base impedance, V_g,V_0= per phase air-gap voltage and output voltage. In Ref. [12] assumptions in the analysis of SEIG is reported and from Fig. 2, the loop equation for the current I is given in (1) and Z is the net loop impedance given by,

$$IZ=0 \tag{1}$$

$$Z = \left[\left(\frac{R_r}{(F-v)} + jX_{lr}\right) \| X_m\right] + \frac{R_s}{F} + jX_{ls} + \left[-\frac{jX_c}{F^2} \| \frac{R}{F} + jX\right] \tag{2}$$

Since under steady-state excitation I ≠ 0, it follows from (1) that Z=0 or both real and imaginary parts of Z are zeroes. For finding general solution for $C_{min,}$ all the coefficients are evaluated at X_m=X_{smax}, where

$$C= 1/2\pi f_b X_c Z_b \tag{3}$$

by simplifying (2), the obtained equation is given by

$$\alpha_4 F^4 - \alpha_3 F^3 + \alpha_2 F^2 - \alpha_1 F + \alpha_0 = 0 \tag{4}$$

Where, i=0, 1…, 4 are positive constants is reported in [15]. By solving **(4)** gives two real roots, the obtained C_{min} = 77μF and C_{max} = 152μF and **(4)** can be rearranged as

$$\alpha_4 F^4 + \alpha_2 F^2 + \alpha_0 = \alpha_3 F^3 + \alpha_1 F. \tag{5}$$

The two curves intersect in the range $F_{min} \leq F \leq F_{max}$, where $\mathbf{C_{min}}$ is estimated by using MATLAB programming. Thus for R-L case two real roots exists where the minimum capacitance value is taken for self-excitation.

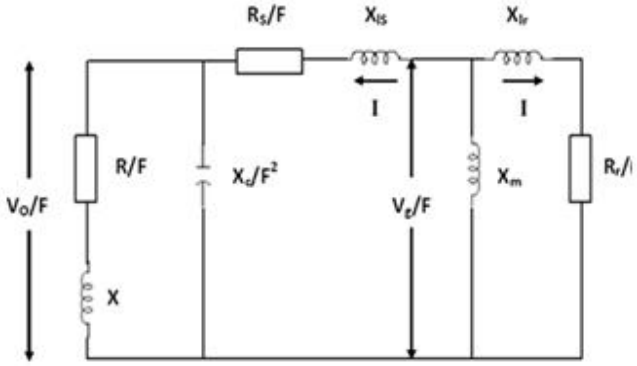

Figure 2.Per unit per phase steady-state equivalent circuit of self-excited induction generator with R-L load

IV. Design Of Electronic Load Controller Components

The voltage rating of the uncontrolled rectifier and the chopper switch will be the same and dependent on the rms ac input voltage and the average value of the output dc voltage. The dc output voltage is calculated as,

$$V_{dc} = \frac{3\sqrt{2}V_{LL}}{\pi} = (1.35) * V_{LL} = 513.8V \tag{6}$$

Where, V_{LL} is the rms value of the SEIG terminal voltage. An overvoltage of 10 percent of the rated voltage is considered for transient conditions and therefore the rms ac input voltage with the peak value is given by (7).

$$V_{peak} = \sqrt{2} * 10\% \text{ of rated voltage} = 580V \tag{7}$$

The ac input peak current and the rating of the dump load resistance (R_D) and the value of dc-link capacitance (C) of the ELC is selected by considering ripple factor (here RF=5%) . In Ref. [15] the ripple factor is 5% and $I_{peak,}$ $R_{D,}$ C is given by,

$$I_{peak} = 2 * P/(\sqrt{3} * V_{LL} * 0.955) = 7A \tag{8}$$

$$R_D = V_{DC}^2 / P_{rated} = 119.7\Omega \tag{9}$$

$$C = (1 / 12 * f * R_D)(1+(1/\sqrt{2} * RF)) = 210.83\mu F \tag{10}$$

DOI: 01.IJEPE.4.1.1122

V. Modeling And Design of Lead-Acid Battery

The ELC of the schematic diagram consists of 3-Φ diode-bridge rectifier fed chopper circuit with dump load along with battery. Instead of wasting the power to the dump load, the battery can be used for charging. The lead acid battery is used in this schematic arrangement, where the discharging and charging model of the lead-acid battery is determined in (11) and (12). By using these equations the lead-acid battery is modeled for the respective values obtained due to variation of consumer load. The lead-acid battery is used here for utilizing the power from the ELC due to the consumer load variation. The battery charges when the RL-load is varied, where, the state of charge (SOC in %), the charging current and the charging voltage of the Lead-Acid battery is obtained.

Discharge model ($i^* > 0$)

$$f_1(it,i^*,i,Exp) = E_o - K(Q.i^*/(Q-it)) - K(Q.it/(Q-it)) + laplace^{-1}(Exp(s).0/Sel(s)) \quad (11)$$

Charge model ($i^* < 0$)

$$f_1(it, i^*, i, Exp) = E_o - K(Q.i^*/(Q-it)) - K(Q.it/(Q-it)) + laplace^{-1}((Exp(s)/Sel(s)(1/s)) \quad (12)$$

VI. Simulation Results

A. The loss of excitation and rise in voltage due to wind speed variation with Constant(R-L) load

The stand-alone wind-driven 3-Φ self-excited induction generator is sensitive to wind speed variations. If the speed is decreased below the threshold of the self-excitation, voltage at machine terminals will disappear. In Fig. 3(a) the simulation result of such a situation of which, variation in wind speed from 7m/s to 7.5m/s of 3-Φ wind-driven SEIG fed to the R-L load is shown, where there is no voltage build-up for wind speed 7m/s from 0 to 1.5 seconds. In Fig. 3(b) the line current is shown for the above condition. This shows that the designed excitation capacitance value of 77μF fails to excite. The increase in wind speed leads to the increase in generated voltage of SEIG.

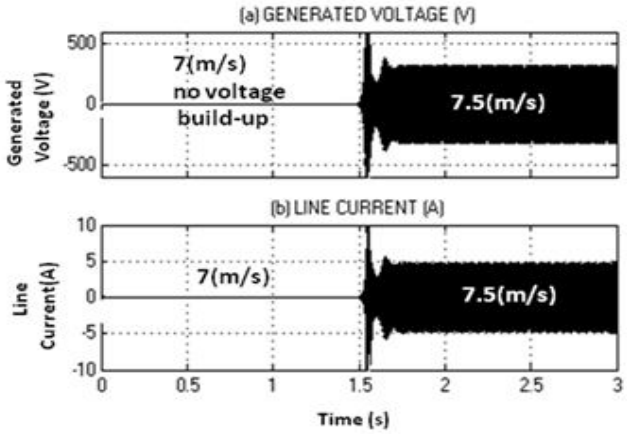

Figure 3. Simulation results of range of wind speed at constant (R-L) load of SEIG (a) Generated voltage (V) (b) Line current (A)

The Fig. 4(c) shows that the increase in speed from 7.5m/s to 10m/s, where the generated voltage increases. From 0 to 1.5 seconds the SEIG runs at 7.5m/s and from 1.5 to 5seconds the SEIG runs at 10m/s. In Fig. 4(d) the line current for the wind speed variation from 7.5m/s to 10m/s is shown.

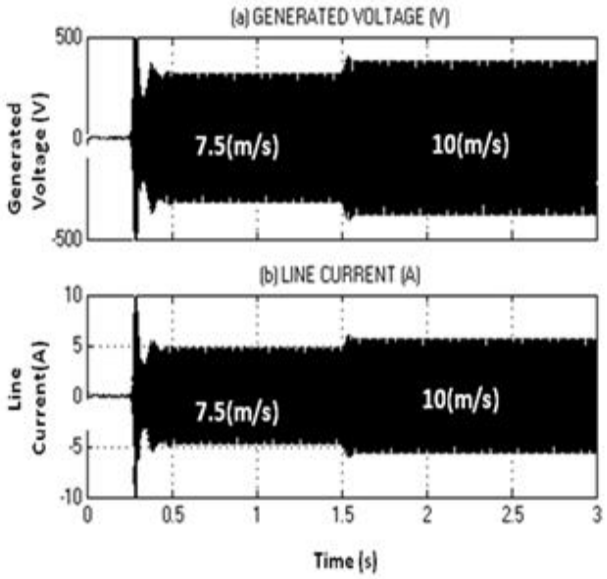

Figure 4. Simulation results of range of wind speed at constant (R-L) load of SEIG (c) Generated voltage (V) (d) Line current (A)

B. Simulation results for 3-$ wind-driven SEIG at varying consumer load with battery storage in closed loop scheme

In closed loop control scheme, the generated ac output voltage of SEIG is converted into equivalent dc voltage by using 3-Ô uncontrolled rectifier which is taken as the reference voltage. When the consumer load is varied from rated load, then the increase in generated voltage is converted into equivalent dc voltage. The dc voltage is compared with the reference voltage, where the output obtained from the comparator is a positive value.

A suitable PI controller is used and the output is compared with triangular waveform and the respective gate signal is given to the chopper switch.

When the chopper switch is switched on, then the current flows through the dump load and the dump load consumes the difference power (generated power-consumer power).

If the comparator output is zero, then the chopper switch is in switched off condition, this shows that the SEIG is operating at the rated (R-L) load. a lead acid battery is connected along with the dump load, where the battery charges, when the chopper is switched on.

In Fig. 5 the generated voltage, the line current, reactive power and real power of SEIG are shown, where SEIG is operated under rated R-L load from 0 to 2.5 seconds and from 2.5 to 5 seconds SEIG is operated under load variation of with constant wind speed 10m/s. In Fig. 6 from 2.5 to 5 seconds the dump load outputs are shown. The Fig. 6 shows the gate pulse for the chopper switch, dump load voltage and dump load current.

The Fig. 7 shows the regulation of voltage at varying R-L load respectively, where the excess voltage is fed to the

DOI: 01.IJEPE.4.1.1122

dump load.

The Fig. 8 shows the simulation results of the dump load along with the lead-acid battery, where (11) and (12) shows the discharge and charge model of lead-acid battery.

From 0 to 2.5 seconds SEIG is operated under rated RL load and from 2.5 to 5 seconds SEIG is operated under load variation with constant wind speed 10m/s, where the power is utilized by using the battery.

The Fig. 8 shows the simulation outputs of charging current, charging voltage, state of charge in (%) of lead acid-battery.

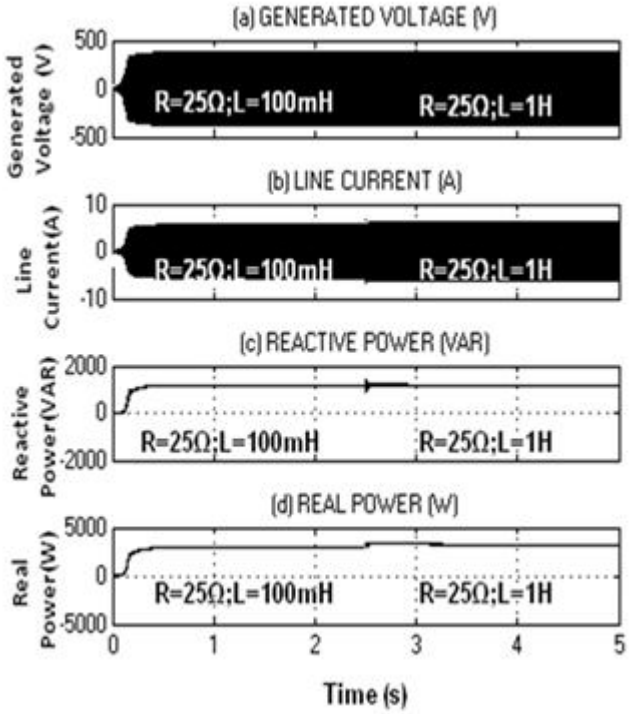

Figure 5. Simulation results of (R-L) load variation of SEIG at constant wind speed (a) Generated voltage (V) (b) Line current (A) (c) Reactive power (VAR) (d) Real power (W)

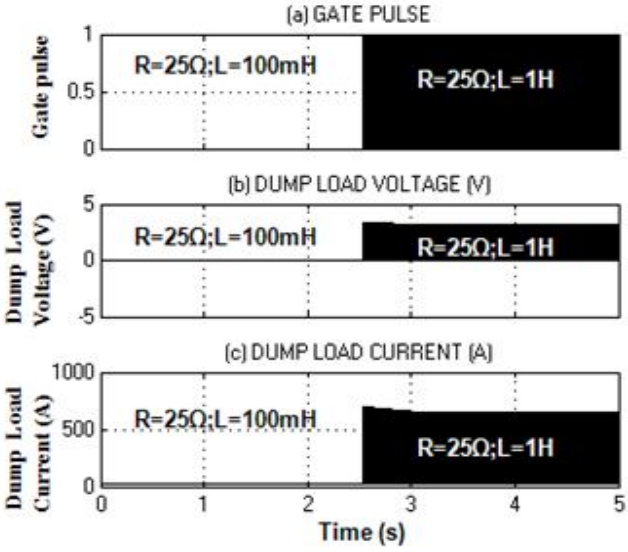

Figure 6. Simulation results of (R-L) load variation of SEIG at constant wind speed (e) Gate pulse (f) Dump load voltage (V) (g) Dump load current

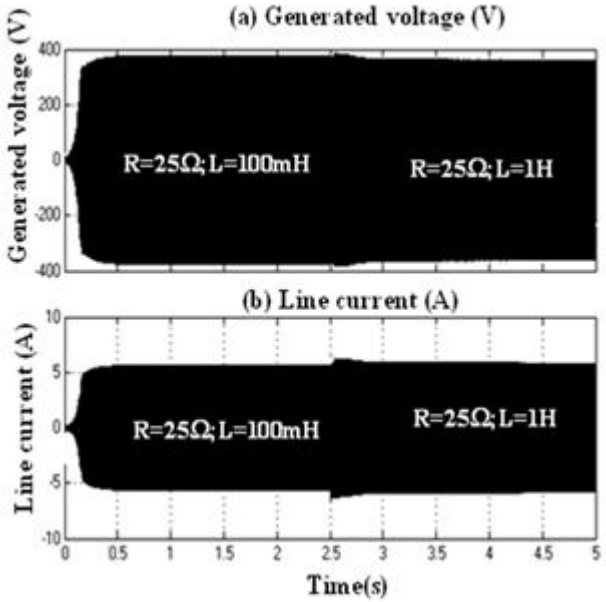

Figure 7.Simulation results of (R-L)load variation of SEIG with battery storage at constant wind speed (a) Generated voltage (V) (b) Line current (A)

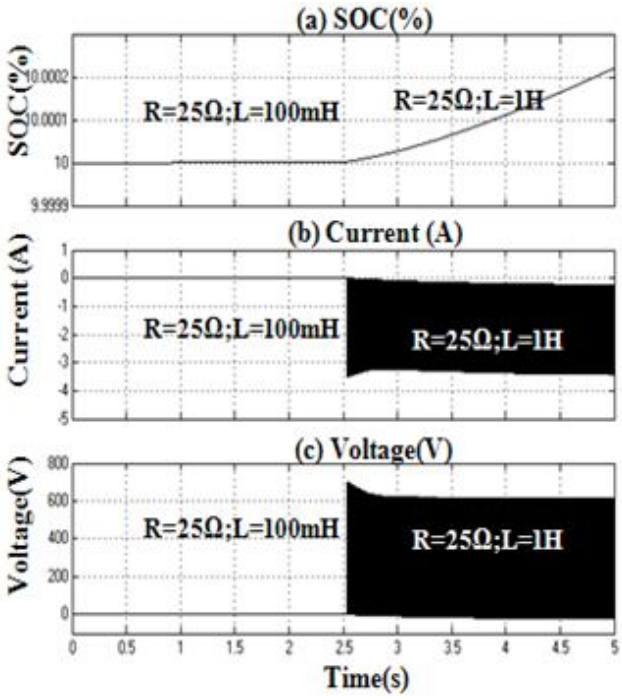

Figure 8. Simulation results of (R-L)load variation of SEIG with battery storage at constant wind speed (a)SOC(%) (b) Current(A)(c)Voltage (V)

C. Simulation results for battery feeding the consumer load in the absence of wind power

The 3- Φ SEIG feeding consumer load, where a lead-acid battery is connected to a 3- Φ voltage source inverter to the consumer load, if there is no wind power. An IGBT switch is used to switch on when there is no wind power. A comparator is used to compare the reference wind speed and the obtained wind speed. If the comparator output is zero, then the switch is in off condition. A filter Land C of values 100mH and 250uF is used for sinusoidal ac output voltage from the inverter.

DOI: 01.IJEPE.4.1.1122

In Fig. 9 the generated voltage and the line current of 3-Φ SEIG under 10m/s and 7m/s of wind speed variation at constant consumer load and the simulation result of lead-acid battery is shown. From 0 to 1second, the 3- Φ SEIG operates at the wind speed of 7m/s, where the 3-Φ SEIG does not generate the voltage.

The Fig. 10 shows gate pulse for battery feeding the consumer load in the absence of wind power. The Fig. 11 shows gate pulse for battery feeding the consumer load in the absence of wind power from 0 to 1 second.

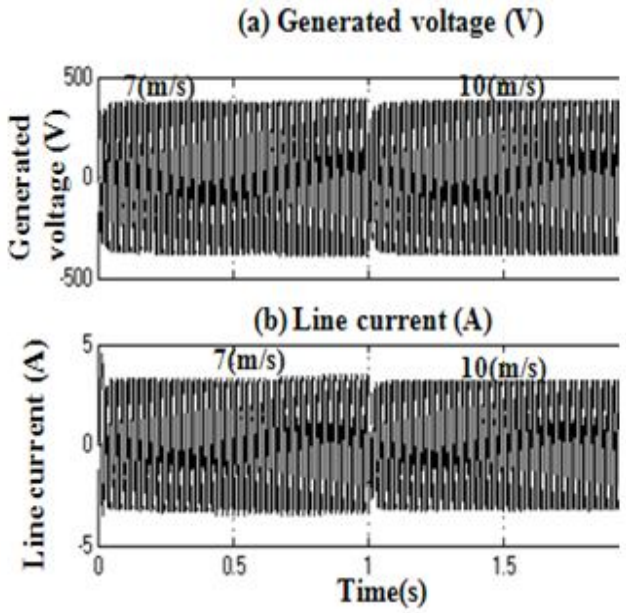

Figure 9. Simulation results for battery feeding the consumer load in the absence of wind power (a) Generated voltage(V) (b) Line current(A)

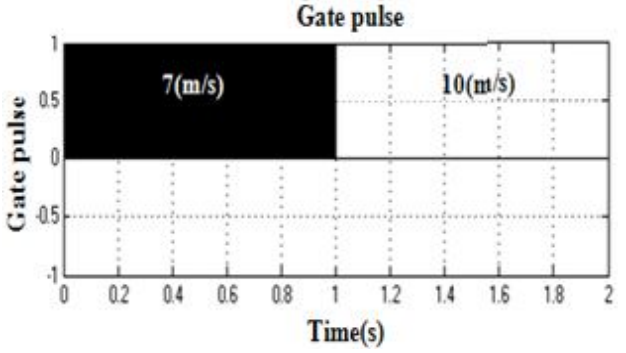

Figure 10. Gate pulse for battery feeding the consumer load in the absence of wind power

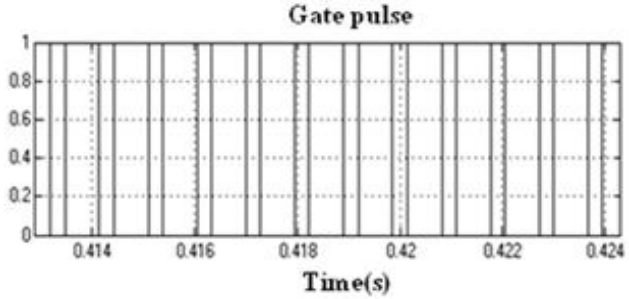

Figure 11. Gate pulse for battery feeding the consumer load in the absence of wind power from 0 to 1 second

Therefore, in Fig. 12 the battery feeds the consumer load, the SOC (%), the battery voltage and the battery current is shown. In Fig. 10, from 1 to 2 seconds the wind speed is 10m/s, where the voltage is generated from the 3-Φ SEIG and feeds the consumer load, where the gate pulse is zero.

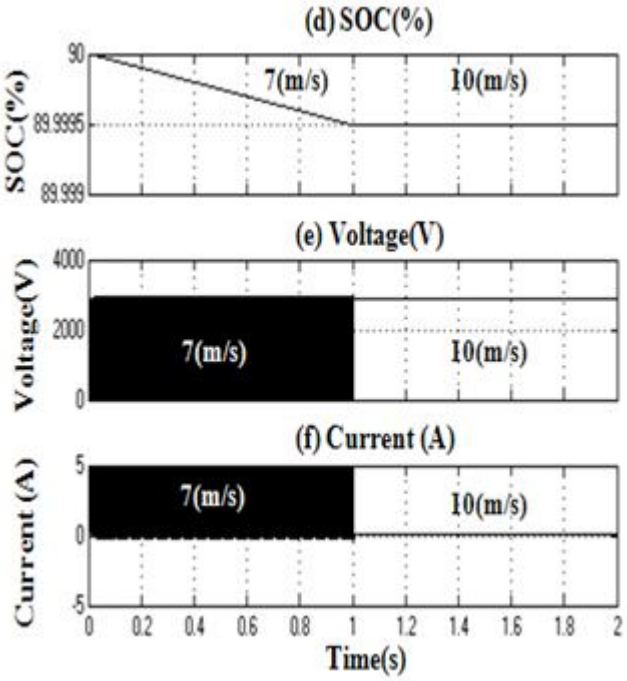

Figure 12. Simulation results for battery feeding the consumer load in the absence of wind power (d) SOC(%) (e) Current(A) (f) Voltage (V)

Conclusions

In this paper, for stand-alone wind driven SEIG with ELC along with the battery storage in closed loop is developed and analyzed. The typical machine and load parameters of the scheme are estimated by the experimental tests undergone in the laboratory and the necessary self-excitation capacitance has been designed mathematically. The design of such a controller in closed loop has been taken up in this work. The range of wind speed variation and the regulation of voltage under the variation of consumer load at constant wind speed are achieved by the developed controller. The real and reactive power requirement for SEIG with ELC is investigated and all simulation results have been presented. The battery feeding the consumer load in the absence of wind power is undergone.

References

[1] Md. Enamul Haque, Michael Negnevitsky and M. Kashem Muttaqi, "A novel control strategy for a variable-speed wind turbine with a permanent-magnet synchronous generator." vol. 46, no. 1, pp. 331-339. Jan-Feb. 2010.

[2] H.R.Van Niekerk,. *Permanent magnet alternators for stand-alone electricity generation*: Department of Electrical and Electronic Engineering, University of Pretoria, Pretoria, 0002. vol. 1, pp. 451-455, Sep.1996.

[3] Rajveer Mittal, K.S. Sandu and D.K.Jain, "Isolated operation

DOI: 01.IJEPE.4.1.1122

of variable speed driven PMSG for wind energy conversion system." *IACSIT International Journal of Engineering and Technolog.*, vol. 1, no.3, August, 2009.

[4] G. Ofualagba, E.U.Ubeku, "The analysis and modelling of a self-excited induction generator driven by a variable speed wind turbine," Federal University of Petroleum Resources, Effurun, Nigeria. *ISBN In Book –Fundamentals and Advanced Ttopics in Wind Power*, vol. 2, pp. 978-953-307-508,June 2011

[5] R.C.Bansal, T.S. Bhatti, D.P.Kothari, "A bibliographical survey on induction generators for application of nonconventional energy systems," *IEEE Trans*. Energy Convers., vol. 18, no. 3, pp. 433–439, Sep.2003.

[6] S.Rajakaruna, R.Bonert, "A technique for the steady-state analysis of a self-excited induction generator with variable speed," *IEEE Trans.Energy Convers.*, vol. 8, no. 4, pp. 757–761, Dec. 1993.

[7] E. Levi, Y.W.Liao, "*An experimental investigation of self-excitation in capacitor excited induction generators."* vol-2, Liverpool L33AF.

[8] N.H.Malik, A.A.Mazi, "Capacitance requirements for isolated self-excited induction generators." vol. 10, pp. 0378-1016, April 1987.

[9] N.H.Malik, S.E.Haque, "Steady state analysis and performance of an isolated self-excited induction generator." vol. 6, no. 9, pp. 38. Jan 2000.

[10] A.K.Jabri, A.I.Alolah, "Capacitance requirement for isolated self-excited induction generator." vol. 137, pp. 154-162, March.1990.

[11] M.Juan Ramirez, M.Emmanuel Torres, "Electronic Load Controller for the Self-Excited Induction Generator." vol. 22, no. 2, June. 2007

[12] B.Singh, S.Murthy, S.Gupta, "Analysis and implementation of an electronic load controller for a self-excited induction generator," *Inst.Electr. Eng. Proc.-Gener. Transm. Distrib.*, vol. 151, no. 1, pp. 51–60, Jan.2004.

DOI: 01.IJEPE.4.1.1122